Improved Thevenin Equivalent Model of MMC Considering Pre-charge Conditions and DC Side Fault Conditions

Enshu Jin [1], Zhenyu Song [1], Xiaofan Yang [2], and Xin Yu [2]

[1] School of Electrical Engineering
Northeast Electric Power University, 169 Changchun Road, Jilin, 132000, China
413115183@qq.com

[2] State Grid Jiangsu Electric Power Co., Ltd.
Yancheng Dafeng District Power Supply Branch, Yancheng, 224000, China
715103343@qq.com

Abstract — The traditional Thevenin equivalent Modular Multilevel Converter (MMC) model has poor versatility for the two working conditions of pre-charging and DC-side faults. In this paper, an improved Thevenin equivalent MMC model considering pre-charge conditions and DC side fault conditions is proposed. The model divides the pre-charging condition into a Controllable charging stage and an Uncontrollable charging stage. The DC-side fault condition is divided into the pre-blocking and post-blocking conditions of the converter. The circuit characteristics are analyzed, and the equivalent model topology is comprehensively improved to make it suitable for full-condition simulation, and a control strategy suitable for the equivalent model is proposed. The detailed model and the proposed improved equivalent model were built in PSCAD/ EMTDC for comparison and analysis. The simulation results shows that the improved equivalent model can be applied to various working conditions, and the versatility of the traditional Thevenin equivalent model is improved.

Index Terms — Converter, electromagnetic transient simulation, improved Thevenin equivalent model, Modular Multilevel Converter (MMC).

I. INTRODUCTION

With the development of modular multilevel converter-based high-voltage direct-current systems (MMC-HVDCs) towards being multi-terminal, high-voltage, and high-power, the number of sub-modules required for MMC bridge arms has increased rapidly. Taking the Dalian Flexible HVDC Transmission Demonstration Project that was put into operation in 2013 as an example, a single bridge arm contains 420 sub-modules (a two-terminal system has 5040 sub-modules). When conducting electromagnetic transient simulations of such a large-scale MMC system, it is necessary to repeatedly invert an ultra-high-order matrix, which makes these simulations extremely slow. Therefore, the traditional detailed MMC electromagnetic transient model is not suitable for the simulation of large-scale MMC-HVDC systems [1–2]. Directly adopting the method of reducing the order of the complex circuit [3] to reduce the order of the detailed model will shorten the simulation time to a certain extent, but the speed-up effect is not good.

In response to the above problems, the establishment of equivalent electromagnetic transient models has gradually become a popular research topic [4]. Among these models, the average-value model [5–13] and the Thevenin equivalent model [1,14–19] are the most widely used. However, the average-value model omits the capacitor voltage balance control module and the circulating current suppression module, so it cannot be used to study the capacitor voltage balance control algorithm or the circulating current suppression strategy [19]. The Thevenin equivalent model has the advantage of being able to inversely resolve the capacitor current and voltage values of the sub-modules while ensuring the accuracy of the simulation. It is therefore used by many electromagnetic transient simulation software packages.

There have been many studies on Thevenin's equivalence. Reference [1] established the equivalent mathematical model of the MMC sub-module based on the Thevenin equivalence theorem. Reference [14] proposed a fast simulation model based on the Dommel equivalent values of capacitance and inductance components, which is only suitable for the normal working conditions of an MMC and not for pre-charging conditions or DC-side fault conditions. In Ref. [15], the insulated-gate bipolar transistor (IGBT) is equivalent, and the sub-module mathematical model under Thevenin's equivalent theorem is constructed; this model has the same shortcomings as the model proposed in Ref. [14], and it has poor versatility. Reference [16] proposed a model based on numerical calculations and a controlled

Submitted On: March 25, 2021
Accepted On: July 7, 2021
https://doi.org/10.47037/2020.ACES.J.360622

voltage source; this model involves detailed numerical calculations, but it requires the establishment of a complex mathematical model to solve the internal parameters of the sub-modules under each fault state, meaning its solution is extremely complicated and unfeasible. Reference [17] proposed a general Thevenin parameter for a single-port sub-module MMC. The calculation method in this report unifies the Thevenin parameter solution process and verifies this based on an MMC with a double half-bridge topology; it has a certain versatility, but it does not give a detailed description of the process of the bridge arm when considering lock-up. Reference [18] extended this general equivalent method to a dual-port sub-module MMC on the basis of Ref. [17], and Ref. [19] further proposed a multi-port method based on Refs. [17] and [18] to produce a general realization method for equivalent models of MMC topology.

The existing Thevenin model still has the shortcoming of poor versatility, and this article will focus on this problem. The specific contributions of this paper include:

1. An analysis of the circuit characteristics of the converter under pre-charge conditions and DC-side fault conditions. Establishing the reason for the poor versatility of the existing Thevenin equivalent model based on the circuit characteristics under these two working conditions. In response to the above problems, improving the equivalent models under these two working conditions.
2. Combining the improved equivalent model under the two working conditions with the traditional Thevenin equivalent model and proposing an equivalent model suitable for full-condition simulations, along with a suitable control strategy.

The remainder of this paper is arranged as follows. Section 2 introduces the traditional Thevenin equivalent model. In Section 3, the circuit characteristics under pre-charge and DC-side fault conditions are analyzed, and the equivalent models under these two conditions are improved. Section 4 integrates the improved equivalent model into the traditional Thevenin equivalent model, and Section 5 presents a verification of the accuracy and speed of the improved simulation model. Finally, conclusions are summarized in Section 6.

II. TRADITIONAL THEVENIN EQUIVALENT MODEL

Figure 1 shows the half-bridge MMC topology. Each phase is divided into upper and lower bridge arms. These bridge arms are composed of the bridge-arm reactors L_0 and N half-bridge sub-modules (HBSMs) in series. To reduce the number of nodes contained in the bridge-arm unit, an adjoint circuit of MMC is established which is shown in Fig. 2. The values of the equivalent resistances R_1 and R_2 of the switching tube branch can be determined according to the IGBT trigger signals TS_1 and TS_2 at time t. The corresponding relationship between the trigger signal state and the value of the equivalent resistance of the switching tube branch is shown in Table 1. As shown, R_{ON}/R_{OFF} represents the ON/OFF resistance of the IGBT and the diode. In PSCAD/EMTDC, the R_{ON} resistance value is generally set to 0.01Ω, and the R_{OFF} resistance value is 10^6Ω.

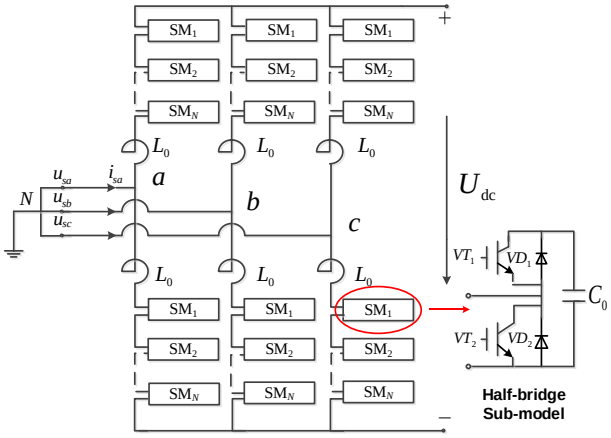

Fig. 1. A MMC and its half-bridge sub-module topology.

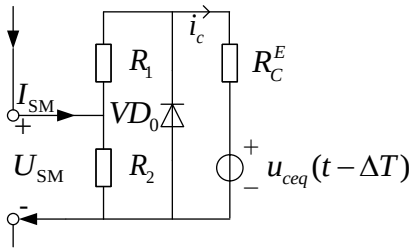

Fig. 2. The adjoint circuit of MMC.

Table 1: Relationship between equivalent resistance of switch tube branch and trigger signal

	Trigger Signal	Switch Tube Branch Equivalent Resistance
Put into	TS_1=1 TS_2=0	R_1=R_{ON} R_2=R_{OFF}
Cut off	TS_1=0 TS_2=1	R_1= R_{OFF} R_2= R_{ON}

Then a Thevenin equivalent model of a single sub-module based on the backward Euler method is established, as shown in Fig. 3 (a), where $R_{smeq}(t)$ is the Thevenin equivalent resistance of the sub-module at time t, as shown in Eq. (1), $U_{smeq}(t)$ is the Thevenin equivalent voltage source at time t, as shown in Eq. (2), and $i_c(t)$ is the current flowing through the sub-module at time t:

$$R_{\text{smeq}}(t)=\begin{cases}\dfrac{\left(R_{ON}+R_C^E\right)\cdot R_{OFF}}{R_{ON}+R_{OFF}+R_C^E} & \text{put into}\\ \dfrac{\left(R_{OFF}+R_C^E\right)\cdot R_{ON}}{R_{ON}+R_{OFF}+R_C^E} & \text{cut off}\end{cases}, \quad (1)$$

$$U_{smeq}(t)=\begin{cases}\dfrac{u_{ceq}\left(t-\Delta T\right)\cdot R_{OFF}}{R_{ON}+R_{OFF}+R_C^E} & \text{put into}\\ \dfrac{u_{ceq}\left(t-\Delta T\right)\cdot R_{ON}}{R_{ON}+R_{OFF}+R_C^E} & \text{cut off}\end{cases}, \quad (2)$$

where R_C^E is the transient equivalent resistance based on the backward Euler method, and ΔT is the simulation step length, $u_{ceq\_i}(t-\Delta T)$ is the equivalent historical voltage source of the capacitor of the sub-module.

Since the turn-off resistance R_{off} of the switch tube group is several orders of magnitude larger than the turn-on resistance R_{on}, to reduce the time for each step updating and calculating the inverse solution during simulation, it is assumed that the turn-off resistance is infinite. Calculate the limit of Eq. (1) and Eq. (2) when R_{off} tends to infinity, which can be simplified as Eq. (3) and Eq. (4):

$$R_{\text{smeq}}(t)=\begin{cases}R_{ON}+R_C^E & \text{put into}\\ R_{ON} & \text{cut off}\end{cases}, \quad (3)$$

$$U_{smeq}(t)=\begin{cases}u_{ceq}\left(t-\Delta T\right) & \text{put into}\\ 0 & \text{cut off}\end{cases}. \quad (4)$$

All the sub-modules on the bridge arm are then superimposed in series to obtain the equivalent model of the traditional MMC bridge arm, as shown in Fig. 3 (b).

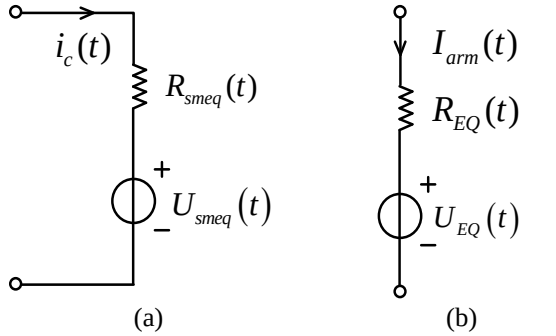

Fig. 3. Thevenin equivalent model of traditional MMC bridge arm, showing (a) sub-module model and (b) bridge-arm model.

In Fig. 3 (b), according to Eq. (3), the equivalent resistance can be obtained using:

$$R_{EQ}(t)=N\cdot R_{\text{on}}+n(t)\cdot R_C^E, \quad (5)$$

where $n(t)$ is the number of sub-modules put into at time t, and N is the total number of sub-modules.

And according to Eq. (4), the equivalent voltage source can be calculated from:

$$U_{EQ}(t)=\sum_{i=1}^{n}u_{ceq\_i}(t-\Delta T). \quad (6)$$

III. IMPROVED THEVENIN EQUIVALENT MODEL

In the traditional Thevenin equivalent model, IGBTs and diodes are not distinguished, and they are treated as switch groups and replaced by variable resistors. Therefore, the traditional Thevenin equivalent model cannot accurately simulate the converter block conditions [20]. The converter will enter a blocked state under pre-charging conditions or DC-side fault conditions. This section will start with these two conditions to improve the traditional Thevenin equivalent model.

A. Pre-charging conditions

Pre-charging of an MMC can be divided into two stages: uncontrollable charging and controllable charging. In the MMC controllable charging stage, the IGBT trigger signal is no longer blocked, and the capacitor can be charged and discharged strategically. At such a time, its equivalent model is consistent with the traditional Thevenin equivalent model, and this will not be repeated here. Here, only the Thevenin equivalent model of the uncontrollable charging stage is improved.

After the converter is blocked during the uncontrollable charging stage, the IGBT is no longer triggered. Figure 4 shows the current-flow path of the MMC bridge arm in the uncontrollable charging stage. It can be seen from the figure that the current only flows through the diodes in the sub-module; the N sub-modules in the same bridge arm that are put into or cut off at the same time are determined by the direction of the bridge-arm current (natural commutation law). At this time, the MMC enters the uncontrollable rectification mode. If the switching time and state variables of this uncontrollable natural turn-off device are not interpolated, then the numerical calculation will produce errors [21]. The accuracy of the traditional Thevenin equivalent model is therefore reduced.

Based on the above analysis, considering the converter structure under the blocking condition, the equivalent model of an HBSM in the uncontrollable charging stage is shown in Fig. 5. First, the Dommel equivalent of the capacitor C_0 is established from an equivalent voltage source and a resistor in series.

The bridge arms are then equalized. Since multiple sub-modules are connected in series on one bridge arm, the bridge arms are equivalent to connecting the equivalent models of their sub-modules in series. Therefore, the improved Thevenin equivalent model of the uncontrollable charging stage can be further established as shown in Fig. 6.

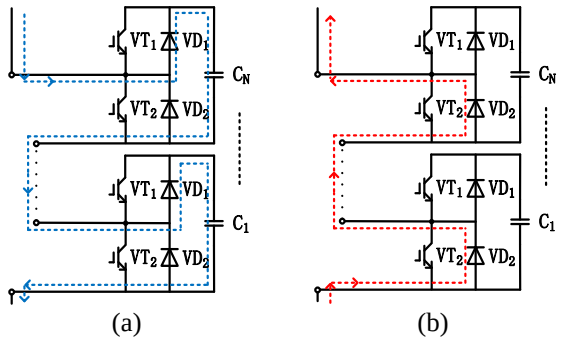

Fig. 4. Current path of MMC bridge arm in the uncontrollable charging stage when (a) Iarm(t) > 0, and (b) Iarm(t) < 0.

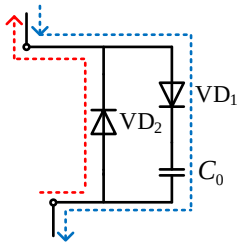

Fig. 5. HBSM Current path of MMC bridge arm in the uncontrollable charging stage.

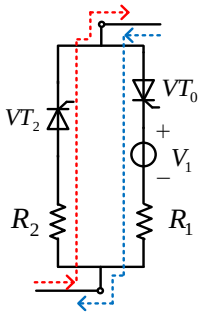

Fig. 6. MMC improved Thevenin equivalent model of the uncontrollable charging stage.

During the uncontrollable charging stage, the controllers VT_0 and VT_2 in the improved Thevenin equivalent model are triggered at the same time. The VT0 branch provides the bridge-arm charging current path, while the VT_2 branch provides a bypass current path. The current is changed due to the uncontrollable charging stage. The phase law is different and flows through the VT_0 or VT_2 branch.

The value of voltage source V_1 in the equivalent model is:

$$V_1(t)=\sum_{i=1}^{N}u_{ceq\_i}(t-\Delta T), \tag{7}$$

the value of the series resistance element R_1 of the VT_0 branch is:

$$R_1=N\cdot\left(R_{on}+R_C^E\right), \tag{8}$$

and the value of the series resistance element R_2 of the VT_2 branch is:

$$R_2=N\cdot R_{on}. \tag{9}$$

B. DC-side fault conditions

In the event of DC-side faults such as single-pole grounding faults and inter-pole short-circuit faults, the MMC can divide the DC-side faults into two stages according to the time scale before and after the converter is blocked due to the time delay of the fault block. The electrical characteristics of the two stages before and after the converter is blocked are different, and the MMC bridge-arm models of the two are also different. Therefore, this section will establish the improved Thevenin equivalent models of the two respective stages.

a. Before the converter is blocked

Each bridge arm of the MMC contains N HBSMs. Before the converter is blocked, each bridge arm still normally switches the sub-modules according to the modulation mode. Suppose n HBSMs are in the on state and $(N-n)$ HBSMs are in the off state; the capacitors of the n on-state sub-modules will bear the DC-side voltage before the converter is blocked. When the capacitors of the n on-state sub-modules are discharged, the discharge current is provided to the short-circuit point through the IGBT devices VT_1 of the n on-state sub-modules and the diodes VD_2 of the $(N-n)$ off-state sub-modules. While the capacitor discharge current is formed, the AC system feeds current through the bridge arm. However, this part of the current is usually negligible before blocking, so this stage is mainly dominated by the capacitor discharge process, and before the converter is blocked, the sub-modules of the bridge arm are switched normally according to the modulation strategy. The MMC bridge-arm model is shown in Fig. 7 (a), and the improved Thevenin equivalent model of the bridge arm before the converter is blocked, as shown in Fig. 7 (b), can be obtained. Here, VT_1 provides a capacitor discharge path. The assignments of the resistance element R_1 and the voltage source V_1 are shown in Eqs. (5) and (6).

b. After the converter is blocked

After the converter is blocked, the capacitor discharge current disappears, and only the AC feed current flows in the bridge arm. The AC feed current path in the bridge arm is shown in Fig. 8 (a), and this flows through all the HBSM diode VD_2 branches in the bridge arm. The improved Thevenin equivalent model after the converter is blocked is shown in Fig. 8 (b). Here, VT_2 triggers to provide an AC feed current path, and the series resistance R_2 of the VT_2 branch is shown in Eq. (9).

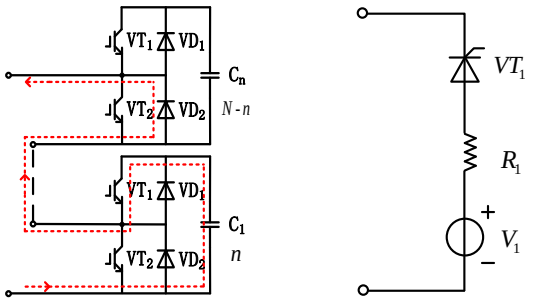

Fig. 7. Equivalent values of MMC bridge arm before converter is blocked, showing (a) capacitor discharge current path, and (b) improved bridge-arm model.

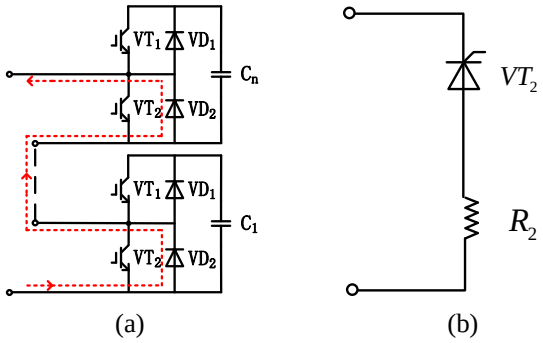

Fig. 8. Equivalent MMC bridge arm after converter is blocked, showing (a) AC feed current path, and (b) improved Thevenin equivalent model.

IV. IMPROVED THEVENIN EQUIVALENT MODEL OF MMC CONSIDERING PRE-CHARGE CONDITIONS AND DC SIDE FAULT CONDITIONS

A. Improved Thevenin equivalent model and it's control strategy

The aforementioned traditional Thevenin equivalent model and the improved Thevenin equivalent model under pre-charge conditions and DC-side fault conditions are combined together, and an improved Thevenin equivalent MMC model considering pre-charge conditions and DC side fault conditions is proposed, as shown in Fig. 9. As shown, the switches k_1, k_2 and k_3 are assigned different switching states under different working conditions of the converter. When the converter is under different working conditions, the calculation formulas for the variable resistors R_1 and R_2 and the controlled voltage source V_1 will change accordingly. The diodes VD_1 and VD_2 ensure unidirectional current flow, and compared with the use of an IGBT, they have the characteristics of simple control. The assignment method for each part is shown in Table 2 (the switch is on when $k(t) = 1$ and the switch is off when $k(t) = 0$).

In view of the improved Thevenin equivalent MMC model proposed in this section, which has considered pre-charge conditions and DC side fault conditions, a suitable control strategy is proposed as shown in Fig. 10. This control strategy can be applied to various operating conditions of the MMC and has the advantages of strong versatility and simple implementation.

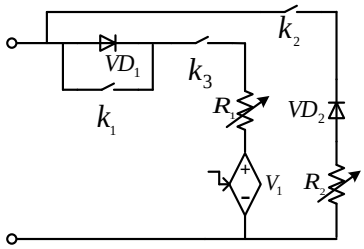

Fig. 9. Improved Thevenin equivalent model of MMC considering pre-charge conditions and DC side fault conditions

Table 2: Assignment method for each part

	①	②		⑤	
		③	④	⑥	⑦
$k_1(t)$	1	1	0	1	0
$k_2(t)$	0	0	1	0	1
$k_3(t)$	1	1	1	1	0
$R_1(t)$	Eq. (5)	Eq. (5)	Eq. (8)	Eq. (5)	*
$R_2(t)$	*	*	Eq. (9)	*	Eq. (7)
$V_1(t)$	Eq. (6)	Eq. (6)	Eq. (7)	Eq. (6)	*

Key: ① normal working condition; ② pre-charging condition; ③ controllable charging; ④ uncontrollable charging; ⑤ DC-fault condition; ⑥ before blocking; ⑦ after blocking.

The modulation strategy uses nearest-level approach modulation, and the control flow is as follows:

1) At the beginning of the simulation (time $t = 0$), the system simulation step ΔT, the initial running values ($i_c(0) = 0$, $u_c(0) = 0$, and $t = \Delta T$), and the sub-module capacitance C_0 will be given. These values are used to calculate the historical voltage source $u_{ceq}(0) = 0$ and the transient equivalent resistance R_C^E of the capacitor. The switch assignment module assigns values to the switches k_1, k_2, and k_3 according to the converter operating conditions.
2) The values calculated in the previous step and the conduction state of each sub-module obtained from the sub-module sorting and selection module are input into the bridge-arm assignment calculation module, and then calculate the variable resistance values $R_1(t)$, $R_2(t)$ and the controlled voltage source voltage value $V_1(t)$.

3) The bridge-arm current $I_{armj}(t)$ is measured after the variable resistance and the controlled voltage source are assigned, and the bridge-arm current can update the current $i_c(t)$ of each sub-module capacitor using:

$$i_c(t)=\begin{cases} I_{arm}(t) & on \\ 0 & off \end{cases}, \quad (10)$$

and the voltage $u_c(t)$ of each sub-module capacitor is then updated.

4) The updated current $i_c(t)$and voltage $u_c(t)$ are used for the next step of calculation, and so on until the end of the simulation.

It should be noted that the sub-module sequence selection module is not put into the control strategy in the Uncontrollable charging stage under the converter pre-charging condition and the post-blocking stage because at this time all the sub-modules in the bridge arm are blocked.

B. Error-calculation formula

We define the average relative error F_1 as:

$$F_1=\frac{\sum_{i=M}^{N}\left|\frac{S_{det}(i)-S_{equ}(i)}{S_{det}(i)}\right|}{\text{N-M}+1}\times 100\%, \quad (11)$$

where $S_{det}(i)$ and $S_{equ}(i)$ indicate data from the i-th sampling point of the detailed model and the equivalent model, respectively, and $i = M, \ldots, N$. We can then define the maximum relative error F_2 as:

$$F_2=\max_i\left|\frac{S_{det}(i)-S_{equ}(i)}{S_{det}(i)}\right|\times 100\% \quad i=M,...,N. \quad (12)$$

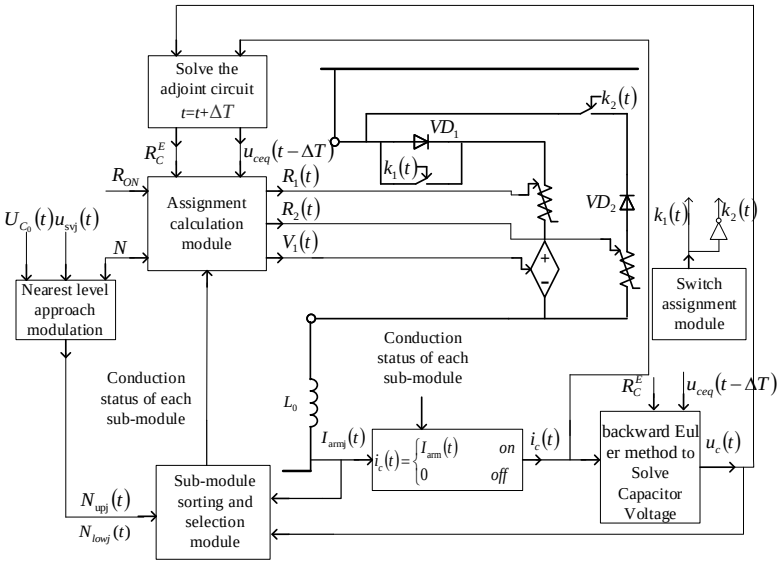

Fig. 10. Control strategy of improved Thevenin equivalent MMC model considering pre-charge conditions and DC side fault conditions.

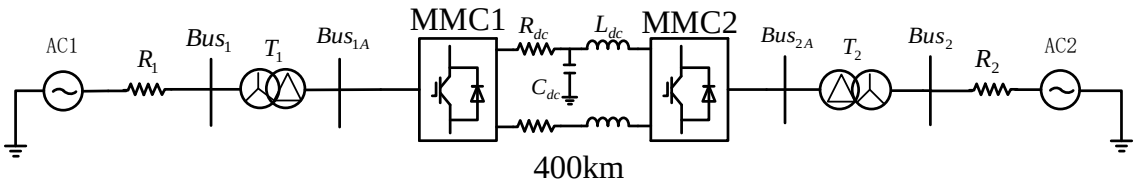

Fig. 11. Diagram of the structure of the simulation system.

V. SIMULATION RESULTS AND ANALYSIS

A double-ended flexible DC-transmission system was built using PSCAD/EMTDC as shown in Fig. 11, where MMC1 and MMC2 are 71-level converters, using detailed models, traditional Thevenin equivalent models, and the improved Thevenin equivalent models proposed in this article. The system parameters are shown in Tables 3–5, and the accuracy and speed of this model are verified in the subsequent sections.

Table 3: Parameters of transformers

Transformer1	Transformer2
S=600MVA	S=600MVA
Ratio=230/245kV	Ratio=230/245kV
X_{T1}=15%	X_{T2}=15%

Table 4: Parameters of DC system

DC Cable	R_{dc}=0.009735 Ω /km
	L_{dc}=0.8489mH/km
	C_{dc}=0.01367uF/km
Length	400km

Table 5: Parameters of AC system

AC System1	AC System2
$V_{BUS1(L-L)}$=230kV	$V_{BUS2(L-L)}$=230kV
R_1=1.67 Ω	R_2=1.67 Ω
SCR=2.5	SCR=2.5

A. Normal working conditions

Figure 12 shows the comparison results of the simulation waveforms of the DC-side voltage, converter power, and the current of the phase-A upper bridge based on the detailed MMC model (Red wide dotted line), the traditional Thevenin equivalent model (blue narrow dotted line), and the improved Thevenin equivalent model proposed in this article (green full line) under normal working conditions of MMC1. Since the improved Thevenin equivalent model is the same as the traditional Thevenin equivalent model under normal working conditions, as shown in Fig. 12, the waveforms of the improved Thevenin equivalent model and the traditional Thevenin equivalent model are consistent with the detailed model waveforms. According to Eq. (11), the average relative errors in the DC voltage, converter power, and phase-A upper-arm current based on the improved Thevenin equivalent model are 0.7912%, 0.5631%, and 0.6347%, respectively. This equivalent model therefore has high simulation accuracy.

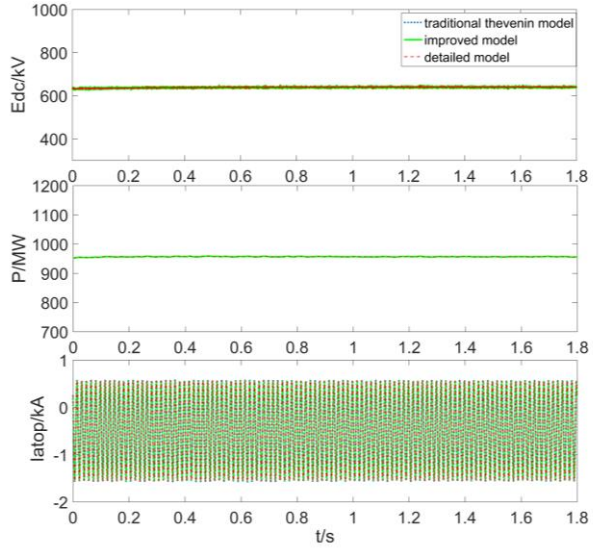

Fig. 12. Simulation comparison results under normal working conditions.

B. Pre-charging conditions

Figure 13 shows the comparison results of the simulation waveforms of the DC-side voltage, converter power, and the current of the phase-A upper bridge on the basis of the detailed model (Red wide dotted line), the traditional Thevenin equivalent model (blue narrow dotted line), and the improved Thevenin equivalent model proposed in this article (green full line) of MMC1 under pre-charging conditions.

It can be seen from Fig. 13 that the traditional Thevenin equivalent model only contains diodes and does not interpolate the switching moments and state variables of this uncontrollable natural turn-off device, resulting in obvious glitches in its waveform compared with the detailed model. According to Eq. (11), the average relative errors of the DC voltage, converter power and phase-A upper-arm current of the traditional Thevenin equivalent model are 0.9872%, 0.9965%, and 1.1254%, respectively, and according to Eq. (12), the maximum relative errors of these three are 4.5123%, 3.9763%, 4.0097%, respectively. The average relative errors in the DC voltage, converter power, and phase-A upper-arm current of the improved Thevenin equivalent model proposed in this article are 0.2214%, 0.2915%, and 0.3123%, respectively, and the maximum relative errors of the three are 0.7234%, 1.2763%, and 1.4547%, respectively. These results are therefore notably closer to the detailed model than the traditional Thevenin equivalent model.

From the above analysis, it can be seen that the improved Thevenin equivalent model has higher simulation accuracy than the traditional Thevenin equivalent model under pre-charging conditions.

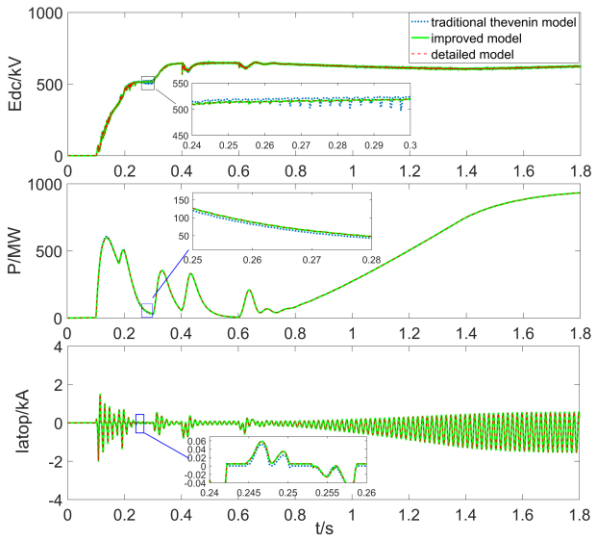

Fig. 13. Simulation comparison results under MMC1 pre-charging conditions.

C. DC-side fault conditions

Figure 14 shows the comparison results of simulation waveforms of the DC-side voltage, converter power, and the current of the phase-A upper bridge based on the detailed model (Red wide dotted line), the traditional Thevenin equivalent model (blue narrow dotted line), and the improved Thevenin equivalent model (green full line) proposed in this article of MMC1 under the condition of a short-circuit fault between the DC-side poles of MMC1.

The occurrence time of the short-circuit fault on the DC side is 0.9 s after the steady state, the fault distance is 0 km to MMC1, the fault is set as a permanent fault, and the system has entered a stable state before the fault occurs. From Eq. (11), the average relative errors of the DC voltage, converter power, and the upper-arm current of phase A of the traditional Thevenin equivalent model are 0.8223%, 0.7146%, and 0.9342%, respectively, and according to Eq. (12), we can get the maximum relative errors of the three as 3.6544%, 1.5643%, and 1.7243%, respectively. The average relative errors of the DC voltage, converter power, and the upper arm current of phase A of the improved Thevenin equivalent model proposed in this article are 0.3231%, 0.6316%, and 0.7667%, respectively, and the maximum relative errors of these three are 0.959%, 0.9261%, and 1.3223%, respectively.

It can be seen from the above data that, compared with the traditional Thevenin equivalent model, the improved Thevenin equivalent model is more consistent with the detailed model and has better simulation accuracy.

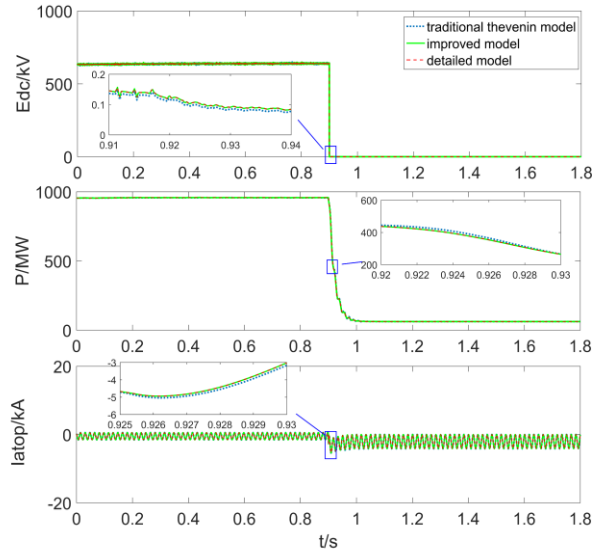

Fig. 14. Comparison of simulation results under a DC-side short-circuit fault.

D. Speed-up effect test

The detailed model, the traditional Thevenin equivalent model, and the improved Thevenin equivalent model proposed in this article of 85-level single-ended MMC were built in PSCAD/EMTDC to verify the speed-up effect. The simulation time is 3s and the step length is 20us. Table 6 shows the comparison results of the running time of the detailed model, traditional Thevenin equivalent model and the improved Thevenin equivalent model; the speedup ratio is defined as the ratio of the running time of the detailed model and the improved Thevenin equivalent model or the traditional Thevenin equivalent model, which is shown in Table 7. From Table 6 and Table 7, it can be seen that the improved Thevenin equivalent model proposed in this paper has the same advantages as the traditional Thevenin equivalent model. When the level number is low, there is no significant difference in the simulation speed of the two equivalent models. When the average number is increased to 85, the speedup ratio of the improved Thevenin model reaches 210.6, and the speedup ratio of the traditional Thevenin equivalent model is 225.64. Although the speed of the improved Thevenin model is slightly slower than the traditional Thevenin equivalent model under the condition of higher level number. However, considering the accuracy advantage of the Thevenin equivalent model mentioned in this article, the slight speed disadvantage is acceptable.

Table 6: Comparison of running times

Number of Levels	Run Time (s)		
	Detailed Model	Traditional Thevenin Model	Improved Equivalent Model
5	13	7	7
11	31	9	9
21	94	11	11
35	423	12	12
85	3159	14	15

Table 7: Speed-up ratio changes with the number of levels

Number of Levels	Speed-up Ratio	
	Traditional Thevenin Model	Improved Equivalent Model
5	1.86	1.86
11	3.4	3.4
21	8.55	8.55
35	35.25	35.25
85	225.64	210.6

VI. CONCLUSION

This study examined the inapplicability of the

traditional Thevenin equivalent model under pre-charge and DC-side fault conditions, and an improved Thevenin equivalent model under the above two conditions was proposed. This was then combined with the traditional Thevenin model under normal operating conditions to create an improved Thevenin equivalent MMC model considering pre-charge conditions and DC side fault conditions. A suitable control strategy for the model was also proposed.

The results of comparisons of simulations using the detailed MMC model, the traditional Thevenin equivalent model, and the improved Thevenin equivalent model proposed in this article showed that the improved Thevenin equivalent model is suitable for pre-charge conditions and DC side fault conditions, has good versatility, high simulation accuracy, and obvious speed-up effects.

VII. COPYRIGHT AND RELEASE INFORMATION

I, the author of the manuscript, declare that there is no conflict of interest exists in the submission of this manuscript, and the manuscript is approved by all authors for publication. I would like to declare on behalf of my co-authors that the work described was original research that has not been published previously, and not under consideration for publication elsewhere, in whole or in part. All the authors listed have approved the manuscript that is enclosed. Your consideration of this article is highly treasured.

ACKNOWLEDGMENT

This work was supported by the National Key Research and Development Program of China (2016YFB0900600); Technology Projects of State Grid Corporation of China (52094017000W).

AUTHOR CONTRIBUTIONS

Enshu Jin: Conceptualization, methodology, analysis, original draft preparation.
Zhenyu Song: Visualization, analysis, software, validation, writing - review & editing, supervision.
Xiaofan Yang: Methodology, software, writing - review & editing.
Xin Yu: Writing - Review & editing, supervision.

REFERENCES

[1] U. N. Gnanarathna, A. M. Gole, and R. P. Jayasinghe, "Efficient modeling of modular multi-level HVDC converters (MMC) on electromagnetic transient simulation programs," in *IEEE Transactions on Power Delivery*, vol. 26, no. 1, pp. 316-324, Jan. 2011.

[2] J. Z. Xu, C. Y. Zhao, and W. J. Liu, "Accelerated model of ultra-large scale MMC in electromagnetic transient simulations," *Proceedings of CSEE, 2013*, vol. 33, no. 10, pp. 114-120, Apr. 2013. (In Chinese).

[3] S. Barmada and A. Musolino, "A new approach for model order reduction of complex circuits," *28th Annual Review of Progress in Applied Computational Electromagnetics, 2012*, pp. 1099-1104, Apr. 2012.

[4] W. H. Chen, M. Z. Wu, J. Zhang, H. Yu, and D. K. Liang, "Review of electromagnetic transient modeling of modular multilevel converters," *Power Syst. Technol., 2020*, vol. 44, no. 12, pp. 4755-4765, Dec. 2020. (In Chinese).

[5] S. S. Khan and E. Tedeschi, "Modeling of MMC for fast and accurate simulation of electromagnetic transients: A review," *Energies, 2017*, vol. 10, no. 8, p. 1161, Aug. 2017.

[6] H. Saad, S. Dennetiere, J. Mahseredjian, P. Delarue, X. Guilaud, J. Peralta, and S. Nguefeu, "Modular multilevel converter models for electromagnetic transients," *IEEE Trans. Power Del., 2014*, vol. 29, no. 3, pp. 1481-1489. Oct. 2014.

[7] H. Zhang, D. Jovcic, W. Lin, and A. J. Far, "Average value MMC model with accurate blocked state and cell charging/discharging dynamics," *4th International Symposium on Environmental Friendly Energies and Applications (EFEA), 2016*, pp. 1-6, Nov. 2016.

[8] J. Z. Xu, A. M. Gole, and C. Y. Zhao, "The use of averaged-value model of modular multilevel converter in DC grid," *IEEE Trans. Power Del., 2015*, vol. 30, no. 2, pp. 519-528. Oct. 2015.

[9] X. Yi, L. Ningcan, X. Zheng, X. Yaowei, and Z. Xinlong, "Simplified transient calculation model in DC-side of VSC-HVDC systems based on MMC average value model," *2014 International Conference on Power System Technology*, pp. 2128-2133, Dec. 2014.

[10] A. Beddard, C. E. Sheridan, and M. Barnes, "Improved accuracy average value models of modular multilevel converters," *IEEE Trans. Power Del., 2016*, vol. 31, no. 5, pp. 2260-2269, May 2016.

[11] X. Y. Pei, G. F. Tang, H. Pang, M. Kong, J. Yang, and Y. N. Wu, "A general modeling approach for the MMC averaged-value model in large-scale DC grid," *2017 IEEE Conference on Energy Internet and Energy System Integration (EI2)*, Beijing, pp. 1-6, Jan. 2018.

[12] S. Nanou and S. Papathanassiou, "Generic average-value modeling of MMC-HVDC links considering sub-module capacitor dynamics," *52nd International Universities Power Engineering Conference (UPEC). IEEE, 2017*, 1-5, Dec. 2017.

[13] H. Y. Yang, Y. F. Dong, and W. H. Li, "Average-value model of modular multilevel converters considering capacitor voltage ripple," *IEEE Trans. Power Del., 2017*, vol. 32, no. 2, pp. 723-732, Apr.

2016.
[14] Y. Zhou and F. Chang, "Quick model of MMC in electromagnetic transient simulations," *Power Syst. Prot. Control, 2016*, vol. 44, no. 1, pp. 1-8, Jan. 2016. (In Chinese).
[15] X. M. Liu, M. H. Li, and J. Zhu, "Research of equivalent mathematical model of MMC sub-modules based on Thevenin's theorem," *Power Syst. Prot. Control, 2016*, vol. 44, no. 1, pp. 1-8, Sep. 2014. (In Chinese).
[16] Yu. F, X. T. Wang, W. X. Lin, and D. Xie, "Fast electromagnetic transient simulation models of modular multilevel converter," *Power Syst. Technol., 2015*, vol. 39, no. 1, pp. 257-263, Jan. 2015. (In Chinese).
[17] Y. C. Zhao, Y. L. Xu, C. Y. Zhao, and J. Z. Xu, "Generalized electromagnetic transient (EMT) equivalent modeling of MMCs with arbitrary single-port sub-module structures," *Proceedings of CSEE, 2018*, vol. 38, no. 16, pp. 4658-4667, Aug. 2018. (In Chinese).
[18] Y. L. Xu, C. Y. Zhao, Y. C. Zhao, L. Shi, and J. Z. Xu, "Generalized electromagnetic transient (EMT) equivalent modeling of MMCs with arbitrary two-port sub-module structures," *Proceedings of CSEE, 2018*, vol. 38, no. 20, pp. 6079-6090, Oct. 2018. (In Chinese).
[19] J. Z. Xu, Y. L. Xu, Y. C. Zhao, and C. Y. Zhao, "Generalized electromagnetic transient equivalent modeling and implementation of MMC with arbitrary multi-type sub-module structures," *Power Syst. Technol., 2019*, vol. 43, no. 6, pp. 2039-2048, June 2019. (In Chinese).
[20] J. Z. Xu, C. Y. Li, Y. Xiong, Y. K. Ji, C. Y. Zhao, and T. An, "A review of efficient modeling methods for modular multilevel converters," *Proceedings of CSEE, 2015*, vol. 35, no. 13, pp. 3381-3392, July 2015. (In Chinese).
[21] C. S. Wang, P. Li, B. B. Huang, L. W. Wang, and F. Gao, "An interpolation algorithm for time-domain simulation of power electronics circuit considering multiple switching events," *J. Electrotech. Technol., 2010*, vol. 25, no. 6, pp. 83-88, June 2010. (In Chinese).

Enshu Jin Professor engaged in research on power system relay protection and electromagnetic transient simulation modeling.

Zhenyu Song Postgraduate engaged in modular multilevel converter modeling and equivalent research work.